

# **The decreasing albedo of the Zhadang glacier on western Nyainqentanglha and the role of light-absorbing impurities**

B. Qu<sup>4,1</sup>, J. Ming<sup>1,2,3</sup>, S.-C. Kang<sup>1,4</sup>, G.-S. Zhang<sup>4</sup>, Y.-W. Li<sup>4</sup>, C.-D. Li<sup>4</sup>, S.-Y. Zhao<sup>5</sup>, Z.-M. Ji<sup>4</sup>, and J.-J. Cao<sup>5</sup>

1 State Key Laboratory of Cryospheric Sciences, Cold and Arid Regions Environmental and Engineering Research Institute, Chinese Academy of Sciences, Lanzhou, China

2 Collaborative Innovation Centre on Forecast and Evaluation of Meteorological Disasters, Nanjing University of Information Science & Technology, Nanjing, China

3 National Climate Centre, China Meteorological Administration (CMA), Beijing, China

4 Key Laboratory of Tibetan Environment Changes and Land surface Processes, Institute of Tibetan Plateau Research, Chinese Academy of Sciences, Beijing, China

5 State Key Laboratory of Loess and Quaternary Geology, Institute of Earth Environment, Chinese Academy of Sciences, Xi'an, China

Corresponding author: J. Ming (petermingjing@hotmail.com)

## Abstract

A large change in albedo has a significant effect on glacier ablation. Atmospheric aerosols (e.g., black carbon (BC) and dust) can reduce the albedo of glaciers and thus contribute to their melting. In this study, two main themes were explored, 1) the decrease in albedo of the Zhadang glacier on Mt. Nyainqentanglha between 2001 and 2012, as observed by the Moderate Resolution Imaging Spectroradiometer (MODIS) on-board the Terra satellite, and the correlation of this albedo with mass balance; and 2) the concentrations of BC and dust in the glacier measured during 2012, and the associated impacts of these impurities on albedo and radiative forcings (RF). The average albedo of the Zhadang glacier from the MODIS increased with the altitude and fluctuated but had a decreasing trend during the period 2001–2012, with the highest (0.722) in 2003 and the lowest (0.597) in 2009 and 2010. The mass balance of the glacier has a positively significant correlation with its surface albedo derived from MODIS. Snow samples were collected in the Zhadang glacier to measure the BC and dust in the summer of 2012. The impacts of BC and dust on albedo reduction in different melting conditions were identified with the SNow ICE Aerosol Radiative (SNICAR) model initiated by in-situ observation data. The sensitivity analysis showed that BC was a major factor in albedo reduction when the glacier was covered by newly fallen snow. Nevertheless, the contribution of dust to albedo reduction can reach as high as 56%, much exceeding that of BC (28%), when the glacier experiences strong surficial melting and its surface was almost bare ice. The average RF caused by dust could increase from 1.1 to 8.6 W m<sup>-2</sup>, exceeding the RF caused by BC after snow was deposited and surface melting occurred in the Zhadang glacier. This implies that it may be dust that primarily dominates the melting of some glaciers in the inner TP during melting seasons, rather than BC.

## 1. Introduction

1   Glaciers and snow cover are important reservoirs of fresh water on Earth. A rough volume of  
2    $2.4 \times 10^7$  km<sup>3</sup> of water is stored in them (Oki and Kanae, 2006), and changes in these  
3   reservoirs have a significant effect on the water supply in many regions of the world (Mote et  
4   al., 2003; Yao et al., 2012). The Tibetan Plateau (TP) is the source of many great rivers (e.g.,  
5   Yangtze, Yellow, Indus, Ganges, and Brahmaputra rivers), which concentrate their sources at  
6   the glaciers in the TP known as the “Asian Water Towers”. More than 1.4 billion people  
7   depend on the water from these rivers (Immerzeel et al., 2010), but these glaciers have been  
8   undergoing rapid changes (Kang et al., 2010; Yao et al., 2012). Therefore, it is important to  
9   understand the impact factors that affect the glaciers and snow cover.

10

11   The surface energy budget of glaciers has significant effects on their ablation (Zhang et al.,  
12   2013), and snow/ice albedo is one of the most important parameters that affect the absorbed  
13   radiation. Snow/ice albedo is defined as the fraction of the reflected and the incident radiant  
14   flux in the surface of the snow/ice. A higher albedo implies a cleaner snow surface or less  
15   energy available for melting. Clean snow has the highest albedo (as high as 0.9) of any natural  
16   substance, but this diminishes when the snow surface is dirty or darkened due to snow grain  
17   size increases (Warren and Wiscombe, 1980; Wiscombe and Warren, 1980). A recent report  
18   (Lhermitte et al., 2012) indicates a darkening surface of the Greenland ice sheet and a rapidly  
19   decreasing albedo during 2000–2011, which will greatly increase the rate of mass loss of the  
20   ice sheet as more solar energy is absorbed by the darker glacial ice (Farmer and Cook, 2013).

21

22   Temperature, precipitation, and glacial dynamic processes are the key factors that affect  
23   glacial change (Sugden and John, 1976). However, there is now a general consensus that  
24   light-absorbing constituents (LACs, e.g., black carbon (BC) and dust) can reduce the albedo  
25   of glaciers (dirtying or darkening effect) and thus also contribute to the mass loss of glaciers.  
26   Both BC and dust are important absorbers of solar radiation in the visible spectrum (Warren  
27   and Wiscombe, 1980; Hadley and Kirchstetter, 2012; IPCC, 2007), and BC has an absorbing  
28   capacity approximately 50 to 200 times greater than dust (Warren and Wiscombe, 1980). The  
29   impacts of BC and dust deposited on the TP glaciers (in particular, on their radiation balance)

30 have been reported in previous literature (Xu et al., 2006; Ming et al., 2009a, 2013a; Lau et al.,  
31 2010; Qian et al., 2011). Simulation of the effect of LACs on the albedo of Himalayan  
32 glaciers showed that LACs in this region had a contribution of 34% to the albedo reduction  
33 during the late spring time, with 21% due to BC and 13% originating from dust (Ming et al.,  
34 2012).

35

36 The lowering of the surface albedo due to the presence of a dust layer could also lead to a  
37 drastic increase in the glacier melting rate during the melting season (Fujita, 2007). In general,  
38 BC can be transported over long distances (Ming et al., 2010; Cao et al., 2010; Kopacz et al.,  
39 2011), whereas dust usually comes from the local or regional environment of the glaciers  
40 (Kang et al., 2000). Historical deposition records of BC revealed by ice cores and lake  
41 sediments over the TP indicate that BC originating from south and central Asia has reached  
42 the glaciers in recent decades (Ming et al., 2008; Xu et al., 2009b; Cong et al., 2013; Wang et  
43 al., 2014).

44

45 There has been extensive research focusing on quantifying the impact of LACs in ice cores  
46 and snow cover to understand the relationship between LACs and albedo reduction (Aoki et  
47 al., 2011; Painter et al., 2007, 2012; Ginot et al., 2013; Kaspari et al., 2013). However, few  
48 researchers discussed the exact effects that BC and dust have on different types of glacier  
49 surfaces during the melting season. Dust sometimes causes significant spatial variation of the  
50 surface albedo in glaciers. Moreover, glacier melting causes LAC particles to concentrate in  
51 the surface and to further enhance the absorption of radiation. This positive feedback  
52 highlights the importance of investigating LACs and their effects on the albedo and glacial  
53 melt across a whole glacier, particularly in the background that the global glaciers are  
54 shrinking in general (IPCC, 2007) and the total BC emission is increasing (Bond et al., 2013).

55

56 The glaciers in the mid Himalaya have been in general darkening since 2000, which is partly  
57 attributed to the deposition of LACs, revealed by a previous study (Ming et al., 2012).  
58 Whereas, the mass balance of the Zhadang glacier in the inner TP was as high as -1500 mm  
59 water equivalent in 2005-2006 (Zhou et al., 2007), experiencing much stronger melting than  
60 Himalayan glaciers. Albedo and the factors inducing the variation of albedo are the “footstone”

61 for understanding the dramatic change of the glaciers. However, the variation of its albedo as  
62 a vital parameter in surface energy budget and the impacting significances of LACs are both  
63 unknown to societies.

64

65 In this work, we will firstly investigate the albedo variation of the Zhadang glacier derived  
66 from the Moderate Resolution Imaging Spectroradiometer (MODIS) on-board the Terra  
67 satellite from 2001 through 2012, and then discuss the spatial distribution of LACs from the  
68 terminate along to the accumulation zone of the Zhadang glacier during the summer of 2012,  
69 and last estimate the contribution of BC and dust to the albedo reduction in different melting  
70 conditions by simulations.

71

## 72 **2. Methodology**

73 The Zhadang glacier is located in western Nyainqentanglha, southern TP, (30°28.57'N,  
74 90°38.71'E, and 5500-5800 m a.s.l.) (Fig. 1). Surface snow/ice samples were collected, and  
75 the surface albedo was observed on the Zhadang glacier during 12-16 July and 24-27 August,  
76 2012. The observation of surface mass balance on the Zhadang glacier has been conducted by  
77 the traditional stake method since late 2005 (Zhou et al., 2007).

78

79 We classified three conditions or scenarios of the glacier surface: (1) S-I: the surface of the  
80 glacier is bare ice containing some visible dark constituents (Fig. 2a); (2) S-II: the surface is  
81 covered by aged snow/firn (Fig. 2a); (3) S-III: the surface is covered by fresh snow (Fig. 2b).  
82 These surface conditions are typical in most alpine glaciers throughout the year (Benn and  
83 Evans, 2010). A description of the sampling details in the Zhadang glacier is given in Table 1.

84

### 85 **2.1 Albedo data from the MODIS**

86 The MODIS albedo data were used to investigate the albedo change in the Zhadang glacier.  
87 The series of the product is the MODIS/Terra Snow Cover Daily L3 Global 500m Grid  
88 (MOD10A1), which is based on a snow mapping algorithm that employs a normalised  
89 difference snow index (NDSI) and other criteria tests (Riggs and Hall, 2011). The MOD10A1  
90 product contains four data layers: snow cover, snow albedo, fractional snow cover, and binary

91 quality assessment (QA), which is assigned as “good” or “bad”. The data are compressed in  
92 hierarchical data format-Earth observing system (HDF-EOS) and are formatted along with the  
93 corresponding metadata. The images of MOD10A1 are 1200 km by 1200 km tiles with a  
94 resolution of 500 m × 500 m gridded in a sinusoidal map projection. Data are available from  
95 24 February 2000 to present via FTP (Hall et al., 2006). The snow albedo data used in the  
96 calculation are based on three expected criteria: the pixels are identified as snow cover,  
97 fractional snow cover is 100, and the pixels pass the QA. The MODIS daily albedo has high  
98 accuracy in flat terrain (Stroeve et al., 2006; Tekeli et al., 2006.), but it shows some errors in  
99 complex topography, such as mountainous regions (Sorman et al., 2007; Warren, 2013).

100

101 To verify the applicability of the MOD10A1 product in the Zhadang glacier, we used the  
102 observed data measured by the Kipp & Zonen radiometers mounted on an automatic weather  
103 station (AWS) that was set in the saddle of the glacier (5680 m a.s.l., Fig. 1). The albedo data  
104 were extracted from the precise pixel in the relevant MODIS image where the AWS was  
105 located. The observed albedos were selected in the local time period of 12:30 to 13:30 LT,  
106 considering the scanning time of the Terra satellite passing over the study area. The  
107 correlation analysis between the MODIS data and the observed data showed a good  
108 relationship at the confidence level of 0.02 (Fig. 3), indicating that it is reasonable to use  
109 MOD10A1 data to study the albedo change of the Zhadang glacier.

110

## 111 **2.2 Field albedo observation**

112 Warren (2013) suggested that it is unlikely to detect the impact of BC on snow albedo by  
113 remote sensing. In this work, a spectroradiometer (Model ASD<sup>®</sup> FS-3) was used to measure  
114 the spectral albedo of the glacier. This covers a radiation waveband of 350-2500 nm with a  
115 wavelength resolution of one nanometre. The optical sensor of the spectroradiometer was set  
116 in a pistol-shape device so that the optical fibre can be fixed inside and mounted on the rocker  
117 arm of the tripod with a gradienter for levelling. The distance between the sensor and the  
118 snow surface was approximately 0.5 m, allowing for the measurement of the spectral  
119 reflectances. Air temperature has been recorded by an autonomous weather station (AWS)  
120 built up in the accumulative zone of the Zhadang glacier since 2008 (Fig. 1).

121

122 During the expedition of July 2012, we measured the surface albedo and collected snow  
123 samples in S-I (two sites: A and B) and S-II (C and D) conditions. In August, the glacier was  
124 covered by newly fallen snow, and the albedo and surface snow samples were successfully  
125 observed and collected at eight sites in S-III conditions (Fig. 2). Along with the sampling,  
126 other necessary parameters, such as snow density, and grain sizes, for simulating the surface  
127 albedo were also observed. Details concerning the simulations of the surface albedo have  
128 been introduced in a previous work (Ming et al., 2013a).

129

### 130 **2.3 Snow/ice sampling and BC/dust measurement**

131 Snow/ice samples were collected in accordance with the “Clean Hands-Dirty Hands”  
132 principle, meaning that the person whose hands are collecting sampling will not touch any  
133 other material that may contaminate the snow samples (Fitzgerald, 1999). We collected two  
134 parallel samples 10 cm away from each other from the surface to 5 cm depth at each site when  
135 measuring the albedo. The snow density was measured using a balance. The samples were  
136 stored in NALGENE® HDPE wide-mouth bottles (250 mL) and were kept frozen until  
137 laboratory analysis. The snow grain sizes were measured using a hand lens (25X) with an  
138 accuracy of 0.02 mm; the largest length of a single ice crystal was also measured using a  
139 snow crystal card with 1 mm grids (Aoki et al., 2007). We filtered the snow melt water  
140 through quartz-fibre filters, which were weighed before and after the filtration using a  
141 microbalance to evaluate the mass of on-load dust. A thermal-optical method of carbon  
142 analysis, using DRI® Model 2001A OC/EC (Chow et al., 1993), was employed to measure the  
143 BC mass in the samples.

144

### 145 **2.4 Albedo reduction modelling and radiative forcing (RF)**

146 The Snow-Ice-Aerosol-Radiative (SNICAR) model can be used to simulate the hemisphere  
147 albedo of snow and ice for unique combinations of impurity contents (BC, dust, and volcanic  
148 ash), snow grain size, and incident solar flux characteristics (Flanner et al., 2007). It was  
149 applied to simulate the albedo variation caused by BC and dust deposited in the glacier  
150 surface in this work. We conducted a series of sensitivity analyses to identify the impact of  
151 BC and dust on albedo reduction in three different surface conditions of the Zhadang glacier  
152 (also see Section 2.2). The solar zenith angle was identified based on the time and position of

153 the specific sampling sites. The snow grain effective radius is taken as half the observed snow  
154 grain size introduced by Aoki et al. (2007) and is shown in Table 1. The albedo of the  
155 underlying bare ice is taken as 0.11-0.19 in the visible band and 0.18-0.23 in the near-infrared  
156 band as measured in-situ by the spectroradiometer. We use the default value 1 as the mass  
157 absorption cross section (MAC) scaling factor (experimental) in the modelling. The detailed  
158 parameters used in SNICAR are listed in the appendix.

159 RF was defined using the equation below,

$$160 \quad RF = R_{in-short} * \Delta\alpha,$$

161 where  $R_{in-short}$  denotes the incident solar radiation measured by radiometer, and  $\Delta\alpha$  denotes the  
162 reduction of the albedo.

163

### 164 **3. Results and Discussion**

#### 165 **3.1 Surface albedo variations of the Zhadang glacier during the period** 166 **2001-2012**

167 The albedo of the Zhadang glacier increased with elevation (Table 1) due to the lower  
168 temperature favouring more cold snow stored in higher elevations. The annual average albedo  
169 from the MODIS decreased from 0.676 in 2001 to 0.597 in 2010 with a maximum of 0.722 in  
170 2003 and a minimum of 0.597 in 2009 and 2010. The albedo of the Zhadang glacier shows an  
171 obvious decreasing trend of  $0.003 \text{ a}^{-1}$  during the period 2001-2012, despite the inter-annual  
172 fluctuations (Fig. 4). This trend was also revealed in the Himalayan and Tanggula glaciers  
173 (Ming et al., 2012; Wang et al., 2012). Regional air temperature shows a decreasing trend  
174 during the period 2008-2012, which seems not to **interpret** the albedo decreasing (Fig. 4),  
175 **implying that other factors could induce the varying.**

176

177 The surface albedo of a specific glacier could be linked with its mass balance in the TP, which  
178 has been proved by Wang et al. (2013). We used the observed mass balance data from 2006  
179 through **2012** in the Zhadang glacier (Zhou et al., 2007; Zhang et al., 2013) to perform a  
180 correlation analysis with the glacier surface albedo (Fig. 4). Lower albedos are related to more  
181 negative mass balances, and vice versa. For example, the most negative mass balance  
182 appeared in 2010 when the albedo reached the minimum, whereas the most positive mass  
183 balance occurred in 2008, and the albedo was also the highest. The significant positive



184 correlation ( $n = 7$ ,  $\alpha = 0.01$ ,  $R^2 > 0.83$ ) between the albedo and the mass balance of the glacier  
185 **implies** that surface albedo is a strong index of the mass balance for the glacier.

186

### 187 **3.2 Impacts of BC and dust on the albedo**

188 A previous study conducted at a site approximate 20 km northeast of the Zhadang glacier  
189 indicated that the BC concentration showed an increasing trend during the period 2006-2010  
190 (Zhao et al., 2013), which allows to presume the possibly increasing deposition of BC in the  
191 glacier surface, enhancing the surficial radiation absorption and decreasing the albedo. Thus  
192 taking LACs into consideration, and sampling and measuring their concentrations are  
193 reasonable for interpreting the albedo decreasing revealed by the MODIS data.

194

195 The measurements of BC and dust concentrations, as well as other observations, such as snow  
196 grain size, snowpack density, and snowpack thickness, on the Zhadang glacier are shown in  
197 Table 1. In S-I conditions, the concentration of dust varied from 504–1892 ppm with an  
198 average of 1198 ppm, whereas BC was 334–473 ppb with an average of 404 ppb. In S-II  
199 conditions, the concentrations of BC and dust ranged from 81 to 143 ppb with an average of  
200 112 ppb and from 34 to 67 ppm with an average of 50 ppm, respectively. However, the  
201 concentration of BC in S-III was 41 to 59 ppb with an average of 52 ppb, whereas the dust  
202 concentration was 3 to 8 ppm with an average of 6 ppm.

203

204 There are large differences in the BC and dust concentrations in the surface of the Zhadang  
205 glacier in different scenarios of surface features (Fig. 2a). In S-I and S-II, intensive surface  
206 melting could lead to a strong enrichment of LACs in the surface of the glacier. In S-III  
207 conditions, the Zhadang glacier was covered by fresh snow due to frequent snowfalls at night  
208 (Fig. 2b). Thus, the concentrations of LACs in S-III are several magnitudes lower than those  
209 in S-I and S-II conditions (Table 1). Table 2 provides observed and simulated albedos at the  
210 sampling sites. The observed surface albedo increases roughly along with the elevation on the  
211 Zhadang glacier, in contrast with the concentrations of BC and dust in S-I and S-II conditions.  
212 The correlations of in-situ observed albedo and the albedo simulated by SNICAR after adding  
213 measured BC and dust into the snow surface are 0.9992 for S-I, 0.9995 for S-II, and 0.4729  
214 for S-III, respectively. This **implies** that the enrichment of BC and dust on the surface of the  
215 glacier could reduce the glacier albedo, thus resulting in the melting of glaciers.

216

217 The sensitivity analysis of the respective impacts of BC and dust on reducing the snow albedo  
218 of the Zhadang glacier was calculated by SNICAR and is shown in Fig. 5. We assume that the  
219 model also works well for thin snow (< 5 cm) with ice beneath. This configuration with the  
220 SNICAR model implies that impurities contained within the ice beneath the snow do not  
221 contribute to the RF calculations. It is unclear how important this assumption is, but it may  
222 contribute to a low bias in the RF estimates. We presume three impacting factors dominating  
223 the albedo varying in the glacial surface, i.e., BC, dust, and the grain size growing due to  
224 warming (Ming et al., 2012). Dust exceeding BC was the most dominant factor in reducing  
225 glacier albedo in S-I. BC other than dust dominates albedo reduction in cases where the  
226 glacier was covered by snow (S-II and S-III). The incoming solar irradiances at every  
227 sampling time during the two trips are listed in Table 2.

228

229 We calculated the RF of both BC and dust on the Zhadang glacier. The simulation shows that  
230 the RF caused by BC and dust deposition on the Zhadang glacier varied between 0.4–11.8 W  
231  $\text{m}^{-2}$  and 0.5–16.4 W  $\text{m}^{-2}$ , respectively (Fig. 5). The RF of dust is much higher than that of BC  
232 in S-I, whereas the RF of BC exceeds dust in S-II and S-III. On average, the forcing caused  
233 by dust deposition on the Zhadang glacier in the summer of 2012 was  $2.7 \pm 3.4$  W  $\text{m}^{-2}$ , and  
234 that caused by BC was  $4.8 \pm 3.2$  W  $\text{m}^{-2}$ , which is a lower than that reported in the northern TP  
235 (Ming et al., 2013b) and higher than reported in the Arctic (Flanner, 2013; Dou et al., 2012).  
236 **Lacking long-term measurements of LACs in the Zhadang glacier makes directly evaluating**  
237 **the impacts of LACs on the albedo decreasing in 2001-2012 impossible, whereas the**  
238 **investigation in 2012 presented a possible interpretation that the LACs could decrease the**  
239 **surface albedo, taking into consideration the increasing of BC concentration in surrounding**  
240 **atmosphere (Zhao et al., 2013).**

241

#### 242 **4. Summary and Conclusions**

243 The albedo of the Zhadang glacier decreased at the rate of  $-0.003 \text{ a}^{-1}$  throughout 2001 to 2012,  
244 according to the MODIS data. The variation of albedo had a positively significant correlation  
245 with the mass-balance variation in 2006-2012, implying that remotely sensed albedo can be  
246 used as an indicating index of the mass balance of the glacier. The deposition of LACs may

247 cause the decreasing of albedo in the Zhadang glacier while the surface temperature showed a  
248 decreasing trend. During the summer of 2012, the average concentrations of BC and dust  
249 were 404 ppb and 1198 ppm in the surface, which are one and three magnitudes higher than  
250 the 52 ppb of BC and the 6.4 ppm of dust in fresh snow of the Zhadang glacier. The impacts  
251 of BC and dust on the glacier albedo were quantified based on the observations and  
252 simulation. The contribution of dust and BC to albedo reduction was 56% and 28%,  
253 respectively, when the glacier was covered by bare ice. In the surface covered by aged snow,  
254 36% of the surface albedo reduction was caused by BC, and 29% by dust. When the glacier  
255 was covered by fresh snow, BC and dust contributed 11% and 3% to albedo reduction,  
256 respectively. In general, BC is a major factor in albedo reduction when the glacier is covered  
257 by fresh and aged snow; however, dust makes the most significant contribution to albedo  
258 reduction when the surface of the glacier is bare ice.

259

## 260 **Acknowledgements**

261 This work was supported by the Global Change Research Program of China (2010CB951401),  
262 the National Natural Science Foundation of China (NSFC Grants 41121001), the State Key  
263 Laboratory of Cryospheric Sciences, CAS (no. SKLCS-ZZ-2012-01-06), CMA (no.  
264 GYHY201106023), the National Science & Technology Pillar Program during the Twelfth  
265 Five-year Plan Period (2012BAC20B05), the Climate Change Science Foundation of CMA  
266 (2013-2014), and the NSFC (Grants 41225002 and 41190081). We would like to thank H.  
267 Zhang for processing the albedo data and appreciate two anonymous referees for their  
268 constructive comments.

269

## 270 **References**

271 Aoki, T., Hori, M., Motoyoshi, H., Tanikawa, T., Hachikubo, A., Sugiura, K., Yasunari, T. J.,  
272 Storvold, R., Eide, H. A., and Stamnes, K.: ADEOS-II/GLI snow/ice products—Part II:  
273 Validation results using GLI and MODIS data, *Remote Sensing of Environment*, 111, 274-290,  
274 10.1016/j.rse.2007.02.035, 2007.

275 Aoki, T., Kuchiki, K., Niwano, M., Kodama, Y., Hosaka, M., and Tanaka, T.: Physically based  
276 snow albedo model for calculating broadband albedos and the solar heating profile in  
277 snowpack for general circulation models, *Journal of Geophysical Research: Atmospheres*  
278 (1984–2012), 116, 2011.

279 Benn, D. I., and Evans, D. J.: *Glaciers and glaciation*, Hodder Education, 2010.

280 Bond, T., Doherty, S., Fahey, D., Forster, P., Berntsen, T., DeAngelo, B., Flanner, M., Ghan, S.,  
281 Kärcher, B., and Koch, D.: Bounding the role of black carbon in the climate system: A  
282 scientific assessment, *Journal of Geophysical Research: Atmospheres*, 10.1002/jgrd.50171,  
283 2013.

284 Cao, J., Tie, X., Xu, B., Zhao, Z., Zhu, C., Li, G., and Liu, S.: *Measuring and modeling black  
285 carbon (BC) contamination in the SE Tibetan Plateau*, *Journal of Atmospheric Chemistry*.  
286 *67(1), 45-60, 2010.*

287 Chow, J. C., Watson, J. G., Pritchett, L. C., Pierson, W. R., Frazier, C. A., and Purcell, R. G.:  
288 The DRI thermal/optical reflectance carbon analysis system: description, evaluation and  
289 applications in US air quality studies, *Atmospheric Environment. Part A. General Topics*, 27,  
290 1185-1201, 1993.

291 Cong, Z., Kang, S., Gao, S., Zhang, Y., Li, Q., and Kawamura, K.: Historical trends of  
292 atmospheric black carbon on Tibetan Plateau as reconstructed from a 150-year lake sediment  
293 record, *Environmental science & technology*, 47(6), 2579-2586, 2013.

294 Dou, T., Xiao, C., Shindell, D., Liu, J., Eleftheriadis, K., Ming, J., and Qin, D.: The  
295 distribution of snow black carbon observed in the Arctic and compared to the GISS-PUCCINI  
296 model, *Atmospheric Chemistry and Physics*, 12, 7995-8007, 2012.

297 Farmer, G. T., and Cook, J.: Earth's Albedo, Radiative Forcing and Climate Change, in:  
298 *Climate Change Science: A Modern Synthesis*, Springer, 217-229, 2013.

299 Fitzgerald, W. F.: Clean hands, dirty hands: Clair Patterson and the aquatic biogeochemistry  
300 of mercury, *Clean Hands, Clair Patterson's Crusade Against Environmental Lead  
301 Contamination*, 119-137, 1999.

302 Flanner, M. G., Zender, C. S., Randerson, J. T., and Rasch, P. J.: Present-day climate forcing  
303 and response from black carbon in snow, *J. Geophys. Res.*, 112, D11202,  
304 10.1029/2006JD008003, 2007.

305 Flanner, M. G.: Arctic climate sensitivity to local black carbon, *Journal of Geophysical  
306 Research: Atmospheres*, 10.1002/jgrd.50176, 2013.

307 Fujita, K.: Effect of dust event timing on glacier runoff: sensitivity analysis for a Tibetan  
308 glacier, *Hydrological Processes*, 21, 2892-2896, 2007.

309 Ginot, P., Dumont, M., Lim, S., Patris, N., Taupin, J., Wagnon, P., Gilbert, A., Arnaud, Y.,  
310 Marinoni, A., and Bonasoni, P.: A 10 yr record of black carbon and dust from Mera Peak ice  
311 core (Nepal): variability and potential impact on Himalayan glacier melting, *Cryosphere*

312 Discussions, 7, 2013.

313 Hall, Dorothy K., George A. Riggs, and Vincent V. Salomonson. MODIS/Terra Snow Cover  
314 Daily L3 Global 500m Grid V005, [January 2001 to December 2010]. Boulder, Colorado  
315 USA: National Snow and Ice Data Centre. Digital media (updated daily), 2006

316 Immerzeel, W. W., van Beek, L. P., and Bierkens, M. F.: Climate change will affect the Asian  
317 water towers, *Science*, 328, 1382-1385, 2010.

318 IPCC, C. C.: The Physical Science Basis. Contribution of Working Group I to the Fourth  
319 Assessment Report of the Intergovernmental Panel on Climate Change, Cambridge University  
320 Press, Cambridge, United Kingdom and New York, NY, USA, 996, 2007, 2007.

321 Kang, S., Wake, C. P., Dahe, Q., Mayewski, P. A., and Tandong, Y.: Monsoon and dust signals  
322 recorded in Dasuopu glacier, Tibetan Plateau, *Journal of Glaciology*, 46, 222-226, 2000.

323 Kang, S., Xu, Y., You, Q., Flügel, W. A., Pepin, N., and Yao, T.: Review of climate and  
324 cryospheric change in the Tibetan Plateau, *Environmental Research Letters*, 5, 015101, 2010.

325 Kaspari, S., Painter, T., Gysel, M., and Schwikowski, M.: Seasonal and elevational variations  
326 of black carbon and dust in snow and ice in the Solu-Khumbu, Nepal and estimated radiative  
327 forcings, *Atmospheric Chemistry and Physics Discussions*, 13, 33491-33521, 2013.

328 [Kopacz, M., Mauzerall, D., Wang, J., Leibensperger, E., Henze, D., and K. Singh: Origin and  
329 radiative forcing of black carbon transported to the Himalayas and Tibetan Plateau,  
330 \*Atmospheric Chemistry and Physics\*. 11\(6\), 2837-2852, 2011.](#)

331 [Lau, W., Kim, M., Kim, K., and W. Lee: Enhanced surface warming and accelerated snow  
332 melt in the Himalayas and Tibetan Plateau induced by absorbing aerosols, \*Environmental  
333 Research Letters\*, 5\(2\), 2010.](#)

334 Lhermitte, S., Greuell, W., van Meijgaard, E., van Oss, R., van den Broeke, M., and van de  
335 Berg, W.: Greenland ice sheet surface albedo: trends in surface properties (2000-2011), EGU  
336 General Assembly Conference Abstracts, 2012, 12349.

337 Ming, J., Cachier, H., Xiao, C., Qin, D., Kang, S., Hou, S., and Xu, J.: Black carbon record  
338 based on a shallow Himalayan ice core and its climatic implications, *Atmospheric Chemistry  
339 and Physics*, 8, 1352, 2008.

340 Ming, J., Xiao, C., Du, Z., and Flanner, M. G.: Black Carbon in snow/ice of west China and  
341 its radiative forcing, *Advances in Climate Change Research*, 92, 114-123, 2009a.

342 Ming, J., Xiao, C. D., Cachier, H., Qin, D. H., Qin, X., Li, Z. Q., and Pu, J. C.: Black Carbon  
343 (BC) in the snow of glaciers in west China and its potential effects on albedos, *Atmospheric  
344 Research*, 92, 114-123, 2009b.

345 Ming, J., Xiao, C., Sun, J., Kang, S., and Bonasoni, P.: Carbonaceous particles in the  
346 atmosphere and precipitation of the Nam Co region, central Tibet, *Journal of Environmental*  
347 *Sciences*, 22, 1748-1756, 2010.

348 Ming, J., Du, Z., Xiao, C., Xu, X., and Zhang, D.: Darkening of the mid-Himalaya glaciers  
349 since 2000 and the potential causes, *Environmental Research Letters*, 7, 014021, 2012.

350 Ming, J., Wang, P., Zhao, S., and Chen, P.: Disturbance of light-absorbing aerosols on the  
351 albedo in a winter snowpack of Central Tibet, *Journal of Environmental Sciences*, 337, 2013a.

352 Ming, J., Xiao, C., Du, Z., and Yang, X.: An Overview of Black Carbon Deposition in High  
353 Asia Glaciers and its Impacts on Radiation Balance, *Advances in Water Resources*, 80-87,  
354 2013b.

355 Mote, P. W., Parson, E. A., Hamlet, A. F., Keeton, W. S., Lettenmaier, D., Mantua, N., Miles,  
356 E. L., Peterson, D. W., Peterson, D. L., and Slaughter, R.: Preparing for climatic change: the  
357 water, salmon, and forests of the Pacific Northwest, *Climatic Change*, 61, 45-88, 2003.

358 Oki, T., and Kanae, S.: Global hydrological cycles and world water resources, *science*, 313,  
359 1068-1072, 2006.

360 Painter, T. H., Barrett, A. P., Landry, C. C., Neff, J. C., Cassidy, M. P., Lawrence, C. R.,  
361 McBride, K. E., and Farmer, G. L.: Impact of disturbed desert soils on duration of mountain  
362 snow cover, *Geophysical Research Letters*, 34, 2007.

363 Painter, T. H., Skiles, S. M., Deems, J. S., Bryant, A. C., and Landry, C. C.: Dust radiative  
364 forcing in snow of the Upper Colorado River Basin: 1. A 6 year record of energy balance,  
365 radiation, and dust concentrations, *Water Resources Research*, 48, 2012.

366 Qian, Y., Flanner, M., Leung, L., and Wang, W.: Sensitivity studies on the impacts of Tibetan  
367 Plateau snowpack pollution on the Asian hydrological cycle and monsoon climate,  
368 *Atmospheric Chemistry and Physics*, 11(5), 1929-1948, 2011.

369 Riggs G, Hall D: MODIS snow and ice products, and their assessment and applications, *Land*  
370 *Remote Sensing and Global Environmental Change*. Springer New York, 681-707, 2011.

371 Sorman, A., Akyürek, Z., Sensoy, A., Sorman, A., and Tekeli, A.: Commentary on comparison  
372 of MODIS snow cover and albedo products with ground observations over the mountainous  
373 terrain of Turkey, *Hydrol. Earth Syst. Sci*, 11, 1353-1360, 2007.

374 Stroeve, J. C., Box, J. E., and Haran, T.: Evaluation of the MODIS (MOD10A1) daily snow  
375 albedo product over the Greenland ice sheet, *Remote Sensing of Environment*, 105, 155-171,  
376 2006.

377 Sugden, D. E., and John, B. S.: Glaciers and landscape: a geomorphological approach,

378 Edward Arnold London, 1976.

379 Tekeli, A. E., Şensoy, A., Şorman, A., Akyürek, Z., and Şorman, Ü.: Accuracy assessment of  
380 MODIS daily snow albedo retrievals with in situ measurements in Karasu basin, Turkey,  
381 Hydrological processes, 20, 705-721, 2006.

382 Wang, M., Xu, B., Cao, J., Tie, X., Wang, H., Zhang, R., Qian, Y., Rasch, P. J., Zhao, S., Wu,  
383 G., Zhao, H., Joswiak, D. R., Li, J., and Xie, Y.: Carbonaceous aerosols recorded in a  
384 Southeastern Tibetan glacier: variations, sources and radiative forcing, *Atmos. Chem. Phys.*  
385 *Discuss.*, 14, 19719-19746, 2014.

386 Wang, J., B. Ye, Y. Cui, X. He, and G. Yang: Spatial and temporal variations of albedo on nine  
387 glaciers in western China from 2000 to 2011, *Hydrol Process.*, doi:10.1002/hyp.9883, 2013

388 Wang, Q., Jacob, D., Fisher, J., Mao, J., Leibensperger, E., Carouge, C., Sager, P., Kondo, Y.,  
389 Jimenez, J., and Cubison, M.: Sources of carbonaceous aerosols and deposited black carbon in  
390 the Arctic in winter-spring: implications for radiative forcing, *Atmospheric Chemistry and*  
391 *Physics*, 11, 12453-12473, 2011.

392 Warren, S.G., Wiscombe, W.J. A model for the spectral albedo of snow. II: Snow containing  
393 atmospheric aerosols. *J. Atmos. Sci* 37, 2734-2745, 1980.

394 Warren, S. G.: Can black carbon in snow be detected by remote sensing?, *Journal of*  
395 *Geophysical Research: Atmospheres*, 118, 779-786, 2013.

396 Wiscombe, W.J., Warren, S.G. A model for the spectral albedo of snow. I: Pure snow. *Journal*  
397 *of the atmospheric sciences* 37, 2712-2733, 1980.

398 Xu, B., Yao, T., Liu, X., and Wang, N.: Elemental and organic carbon measurements with a  
399 two-step heating gas chromatography system in snow samples from the Tibetan Plateau, *Ann.*  
400 *Glaciol.*, 43(1), 257-262, 2006.

401 Xu, B., Cao, J., Hansen, J., Yao, T., Joswia, D. R., Wang, N., Wu, G., Wang, M., Zhao, H., and  
402 Yang, W.: Black soot and the survival of Tibetan glaciers, *Proceedings of the National*  
403 *Academy of Sciences*, 106, 22114-22118, 2009a.

404 Xu, B., Wang, M., Joswiak, D. R., Cao, J. J., Yao, T. D., Wu, G. J., Yang, W., and Zhao, H. B.:  
405 Deposition of anthropogenic aerosols in a southeastern Tibetan glacier, *J. Geophys. Res.*, 114,  
406 D17209, 10.1029/2008JD011510, 2009b.

407 Xu, B., Cao, J., Joswiak, D. R., Liu, X., Zhao, H., and He, J.: Post-depositional enrichment of  
408 black soot in snow-pack and accelerated melting of Tibetan glaciers, *Environmental Research*  
409 *Letters*, 7, 014022, 2012.

410 Yao, T., Thompson, L., Yang, W., Yu, W., Gao, Y., Guo, X., Yang, X., Duan, K., Zhao, H., and

411 Xu, B.: Different glacier status with atmospheric circulations in Tibetan Plateau and  
412 surroundings, *Nature Climate Change*, 2, 663-667, 2012.

413 Zhang, G., Kang, S., Fujita, K., Huintjes, E., Xu, J., Yamazaki, T., Haginoya, S., Wei, Y.,  
414 Scherer, D., and Schneider, C.: Energy and mass balance of Zhadang glacier surface, central  
415 Tibetan Plateau, *Journal of Glaciology*, 59, 137-148, 2013.

416 Zhao, S., Ming, J., Sun, J., and Xiao, C.: Observation of carbonaceous aerosols during  
417 2006-2009 in Nyainqentanglha Mountains and the implications for glaciers, *Environmental*  
418 *Science and Pollution Research*, 20(8), 5827-5838, 2013.

419 Zhou, G., Yao, T., Kang, S., Pu, J., Tian, L., and Yang, W.: Mass balance of the Zhadang  
420 glacier in the central Tibetan Plateau, *Journal of Glaciology and Geocryology (Chinese with*  
421 *English abstract)*, 29(3), 360-365, 2007.



**Table 1.** Sampling information: Two expeditions were conducted on the Zhadang glacier, and samples (albedo, snow/ice) were collected under three melting conditions of the glacier in July and August of 2012. We measured the albedo five to six times at each site whilst collecting two to three snow/ice samples. In total, 120 albedo measurements and 48 snow/ice samples were obtained at the A - D sample sites in July, 2012 for the S-I and S-II conditions (Fig. 2). A total of 160 albedo samples and 64 snow samples were obtained at all sampling sites in August 2012. The albedo and concentrations of BC and dust are listed here.

Sample date	Sample site	Altitude (m a.s.l.)	Number of samples (albedo/snow & ice)	Average of albedo	Average of BC conc. (ppb)	Average of dust conc. (ppm)	Snow grain size (mm)	Snowpack density (kg/m <sup>3</sup> )	Snowpack Thickness (cm)	Solar zenith angle (°)	Cloud Amount (10=100%)	Scene type
July, 2012	A	5507	30/12	0.385	472.6	503.8	0.8 ~ 1.6	289 ~ 380	1	44.8~78.9	3~10	S-I
	B	5680	30/12	0.521	334.4	1891.9	0.6 ~ 1.6	289 ~ 350	1~2	52.3~75.8	1~10	
	C	5720	30/12	0.676	142.9	66.6	0.4 ~ 0.7	333 ~ 378	2~3	62.9~79.1	1~10	S-II
	D	5795	30/12	0.686	80.9	33.6	0.3 ~ 0.5	267~ 289	3	67.1~67.3	0~10	
August, 2012	A	5507	20/8	0.589	53.2	8.2	0.2 ~ 0.5	278 ~ 300	1~2	33.4~44	0~10	S-III
	B	5560	20/8	0.696	40.8	8.0	0.2 ~ 0.4	256 ~ 289	2~3	37.6~47.1	1~7	
	C	5626	20/8	0.710	55.5	7.0	0.2 ~ 0.4	267~ 311	2~3	40.8~50.2	0~7	
	D	5680	20/8	0.699	52.7	6.7	0.2 ~ 0.4	267~289	3	43.8~54.1	1~8	
	E	5695	20/8	0.708	55.2	6.4	0.2 ~ 0.4	267~289	3~4	45.8~57.9	0~6	
	F	5715	20/8	0.667	57.7	6.2	0.2 ~ 0.4	278~289	4	49.9~61.4	0~7	
	G	5750	20/8	0.698	59.4	5.2	0.2 ~ 0.3	222~244	5	51.9~64.6	0~7	
	H	5795	20/8	0.724	40.9	3.4	0.2 ~ 0.3	211~222	5	61.2~68.4	0~10	

**Table 2.** Sensitivity analysis with the SNICAR model. BC% and dust% are the contributions of BC and dust to the total reduction of the albedo, respectively.  $R_{in-short}$  is the incident solar radiation measured by AWS.

Date	Site	OA*	SA** pure	SA +BC	SA +BC & dust	BC%	dust%	$R_{in-short}$	RF +BC	RF +dust	Scene type
15 July	A	0.385	0.406	0.395	0.388	52	33	780.1	8.6	5.5	S-I
16 July	A	0.387	0.413	0.405	0.396	31	34	412.6	3.3	3.7	
15 July	B	0.363	0.406	0.394	0.364	28	70	548.2	6.6	16.4	
16 July	B	0.558	0.577	0.576	0.560	4	85	535.3	0.4	8.6	
14 July	C	0.618	0.640	0.631	0.624	41	32	1308.5	11.8	9.2	S-II
15 July	C	0.723	0.758	0.742	0.727	46	43	543.7	8.7	8.2	
16 July	C	0.745	0.756	0.754	0.752	18	18	604.4	1.2	1.2	
14 July	D	0.745	0.771	0.760	0.753	42	27	552.7	6.1	3.9	
15 July	D	0.732	0.754	0.745	0.740	41	23	648.4	5.8	3.2	
16 July	D	0.755	0.775	0.770	0.764	25	30	789.8	3.9	4.7	
24 Aug	A	0.568	0.791	0.786	0.784	2	1	337.8	1.4	0.7	S-III
25 Aug	A	0.653	0.682	0.681	0.680	5	2	658.7	0.9	0.5	
26 Aug	A	0.716	0.746	0.739	0.737	23	7	702.5	4.9	1.4	
24 Aug	B	0.759	0.793	0.779	0.778	41	4	608.1	8.5	0.9	
25 Aug	B	0.696	0.731	0.728	0.727	8	4	722.7	1.9	0.9	
26 Aug	B	0.656	0.683	0.681	0.68	7	4	736.2	1.5	0.7	
26 Aug	C	0.697	0.734	0.732	0.732	5	1	776.8	1.6	0.3	
24 Aug	D	0.726	0.806	0.797	0.795	11	3	822.6	7.4	1.6	
25 Aug	D	0.768	0.781	0.780	0.778	17	10	814	1.8	1.1	
26 Aug	D	0.647	0.781	0.779	0.778	1	1	811	1.3	1.0	
24 Aug	E	0.699	0.810	0.803	0.802	6	1	962	6.7	1.0	
25 Aug	E	0.780	0.813	0.809	0.807	12	6	891.5	3.6	1.8	
26 Aug	E	0.774	0.811	0.805	0.804	16	3	831	5.0	1.0	
24 Aug	F	0.792	0.839	0.835	0.833	9	4	786.8	3.1	1.6	
25 Aug	F	0.790	0.819	0.816	0.815	10	3	1030	3.1	1.0	
26 Aug	F	0.566	0.816	0.809	0.808	3	1	895	6.0	1.2	
24 Aug	G	0.795	0.848	0.840	0.838	15	4	1303	10.4	2.6	
25 Aug	G	0.806	0.828	0.824	0.823	18	5	1168	4.7	1.2	
26 Aug	G	0.652	0.819	0.812	0.811	4	1	932	6.5	0.9	
24 Aug	H	0.811	0.853	0.846	0.846	16	1	1134	7.5	0.6	
25 Aug	H	0.809	0.834	0.831	0.830	12	4	1316	3.9	1.3	
26 Aug	H	0.711	0.827	0.825	0.824	2	1	1192	2.4	1.2	
Avg.	S-I,II,III	0.684	0.741	0.735	0.731	18	15	826.1	4.7	2.8	

\* OA denotes observed albedo. \*\* SA denotes simulated albedo.

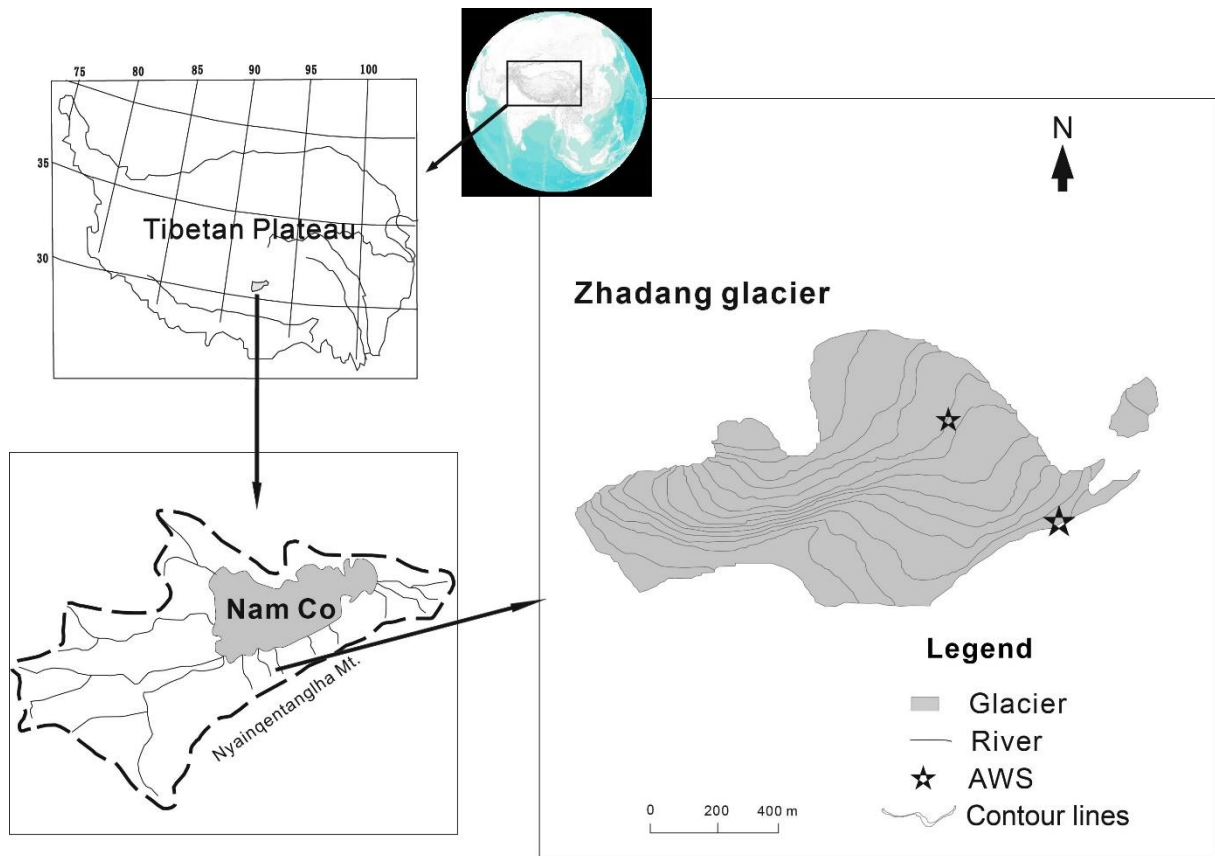


**Fig. 1.** Location of the Zhadang glacier on Mt. Nyainqentangha.

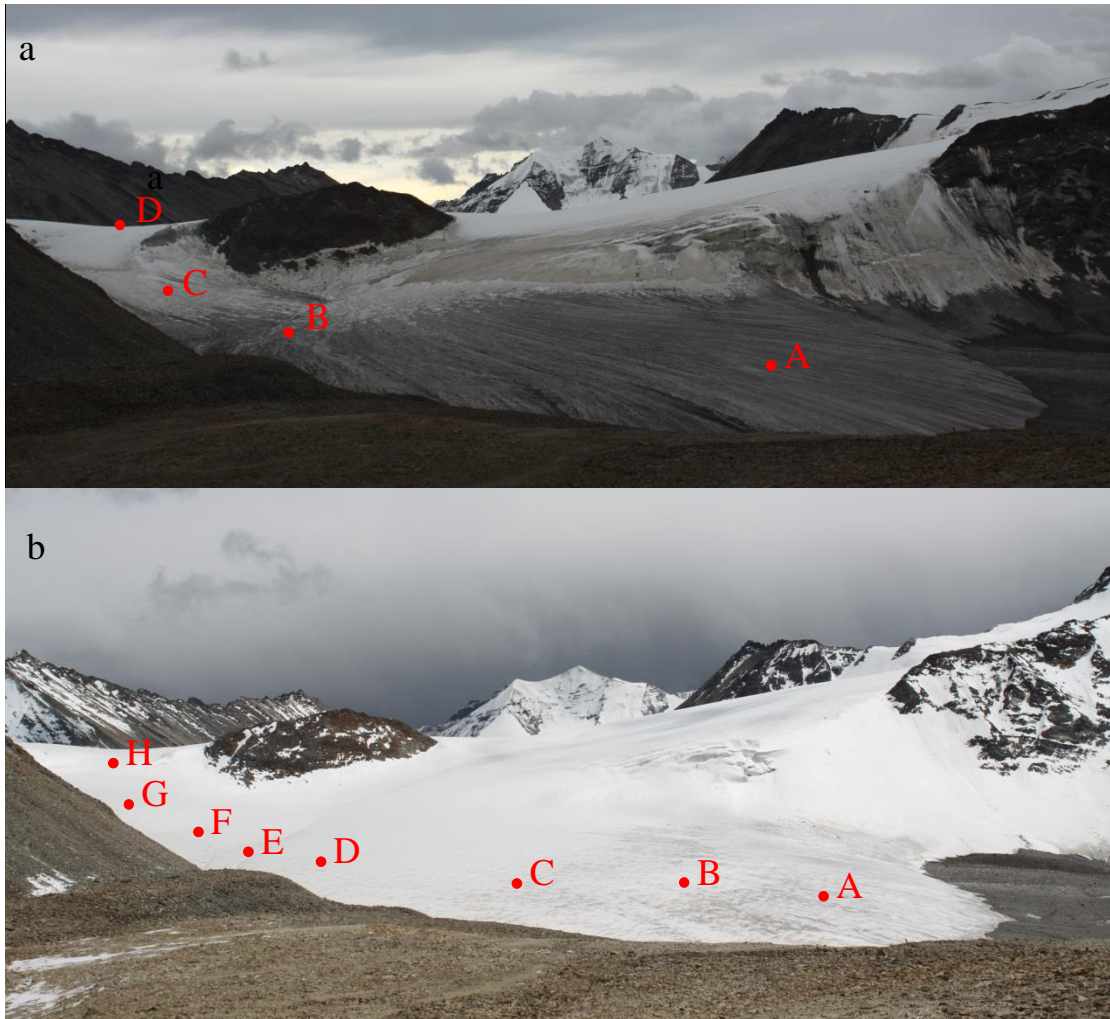


**Fig. 2.** Surface features of the Zhadang glacier on 16<sup>th</sup> Jul. (a) and 26<sup>th</sup> Aug. (b). The two surface conditions include three types of melting conditions: S-I: Sites A and B, which are located in the superimposed ice belt (Fig. 2a); S-II: Sites C and D, which are in the upper area of the glacier (Fig. 2a); S-III: All sites were covered by fresh snow (Fig. 2b).

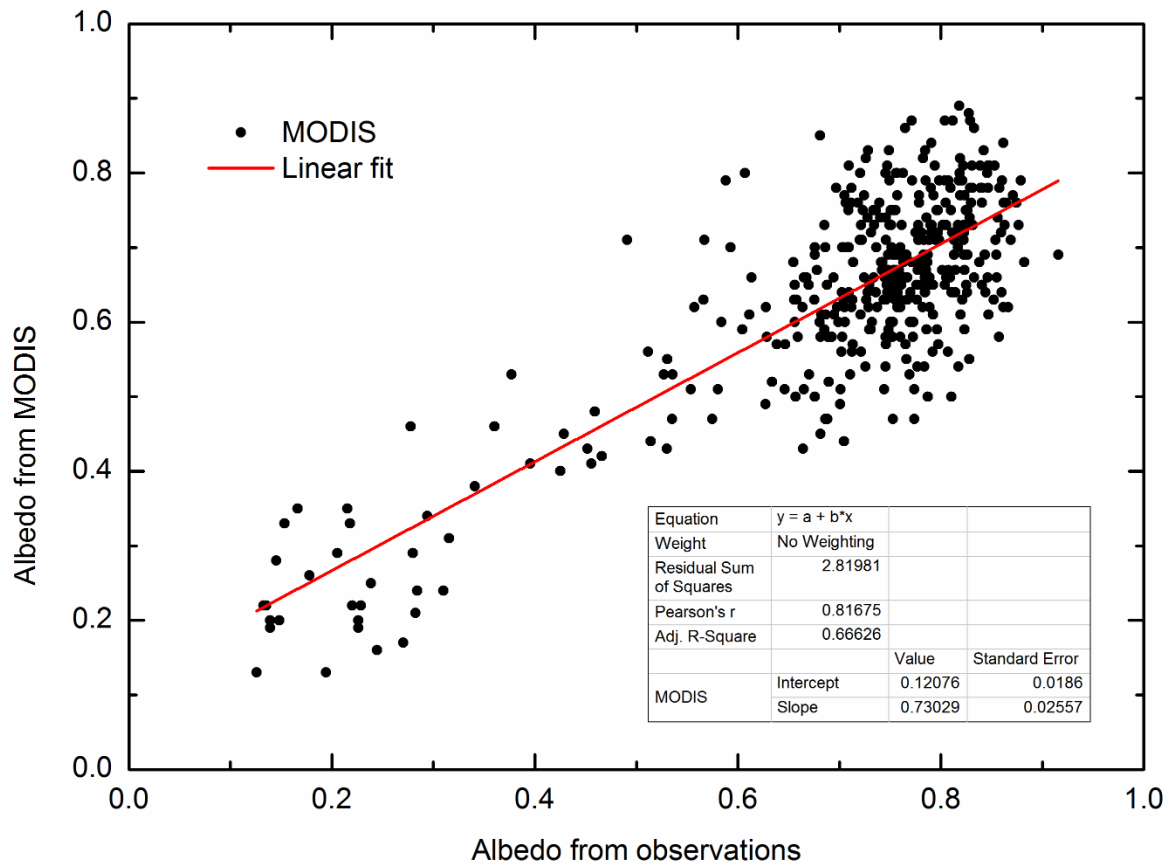


**Fig. 3.** The albedo of the pixel including the AWS in Zhadang glacier derived from MODIS and that observed by AWS in 2011.

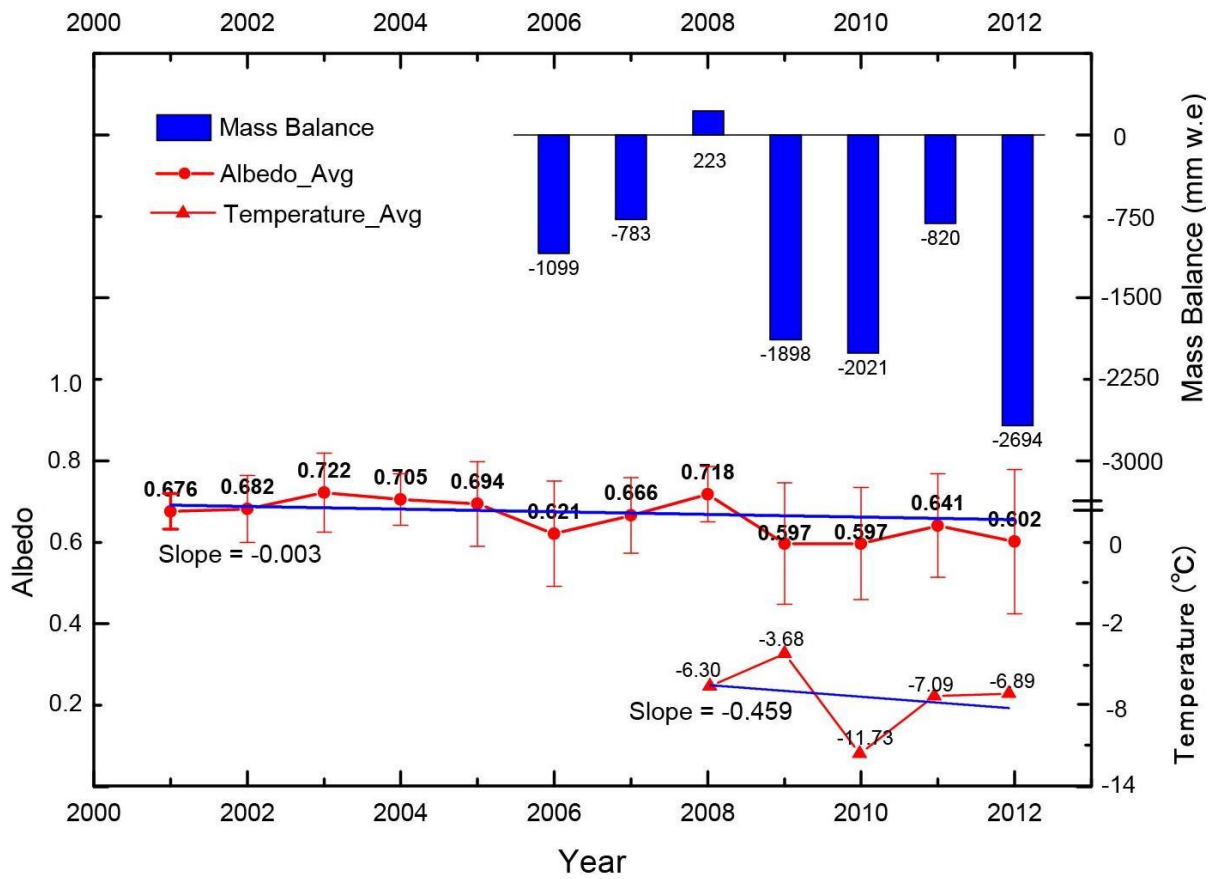


**Fig. 4.** Temporal changes of the albedo in the Zhadang glacier from 2001 to 2012 and the mass balance from 2006 to 2012. The albedo of the Zhadang glacier showed an overall downward trend in the last decade. Air temperature recorded by an AWS in the Zhadang glacier shows a slight decreasing trend.

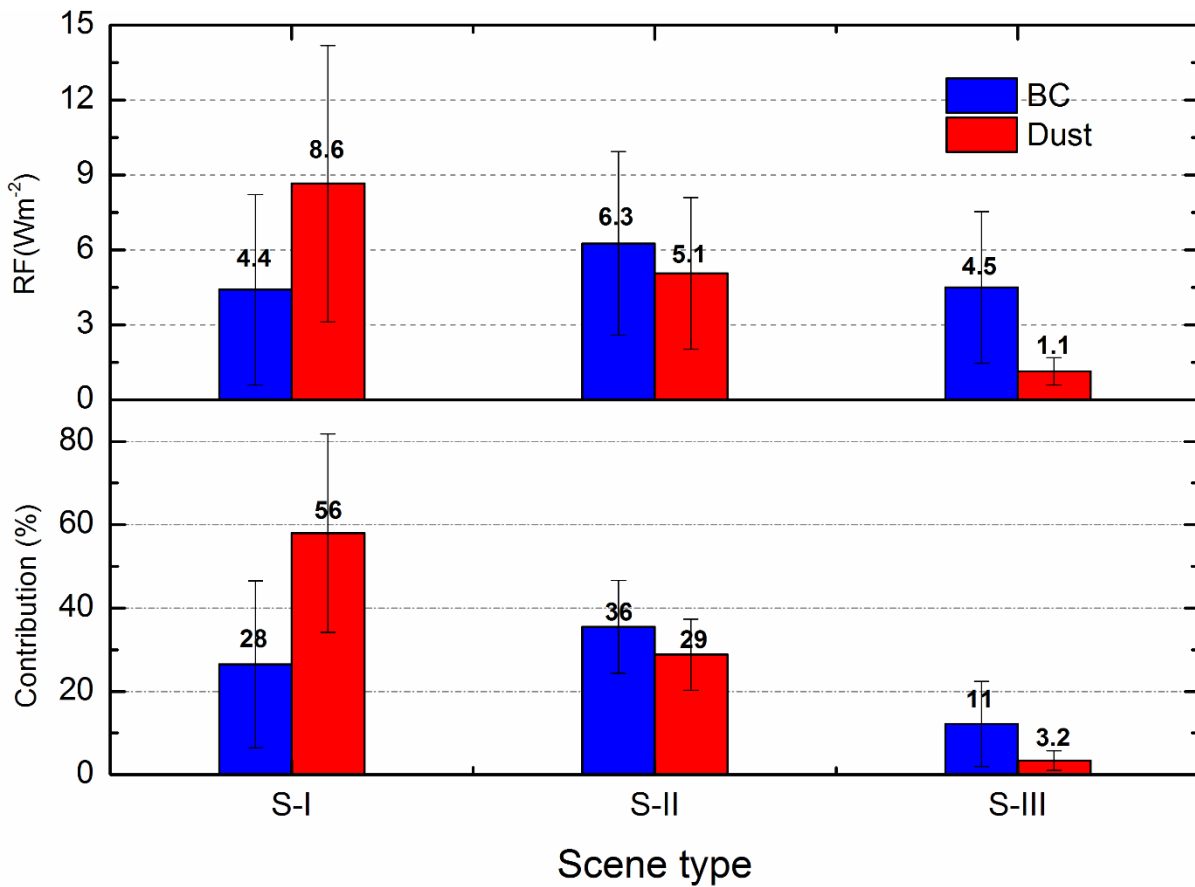


**Fig. 5.** Mid-day RFs of BC and dust on the Zhadang glacier and the contribution (results from the SNICAR model) show the reduction of the albedo in the surface snow cover area under three different melting conditions: S-I, where the surface of the glacier is bare ice; S-II, where the glacier is covered by aged snow; S-III, where the glacier is covered by fresh snow. **Error bars show the uncertainties.**

## Appendix

### Parameters for sensitivity analysis with SNICAR

1. Incident radiation (a. Direct, b. Diffuse); 2. Solar zenith angle; 3. Surface spectral distribution (a. Mid-latitude winter, clear-sky, cloud amount < 5. b. Mid-latitude winter, cloudy, cloud amount  $\geq$  5); 4. Snow grain effective radius ( $\mu\text{m}$ ); 5. Snowpack thickness (m); 6. Snowpack density ( $\text{kg}/\text{m}^3$ ); 7. Albedo of underlying ground (a. Visible, 0.3–0.7  $\mu\text{m}$ . b. Near-infrared, 0.7–5.0  $\mu\text{m}$ ); 8. MAC scaling factor (experimental) for BC; 9. BC concentration (ppb, Sulphate-coated); 10. Dust concentration (ppm, 5.0–10.0  $\mu\text{m}$  diameter); 11. Volcanic ash concentration (ppm); 12. Experimental particle 1 concentration (ppb)

Date	site	1	2	3	4	5	6	7a	7b	8	9	10	11	12
14, July	C	b	79.1	b	600	0.02	378	0.15	0.3	11	129.9	56.4	0	0
14, July	D	b	67.3	b	400	0.05	289	0.15	0.3	11	77.2	29.6	0	0
15, July	A	b	78.9	b	800	0.01	289	0.13	0.12	11	608.2	649.3	0	0
15, July	B	b	75.8	b	800	0.01	289	0.13	0.12	11	657.3	3628.8	0	0
15, July	C	a	71.6	a	400	0.02	367	0.15	0.3	11	278	135.1	0	0
15, July	D	a	67.2	a	400	0.03	278	0.15	0.3	11	114	39	0	0
16, July	A	a	44.8	a	700	0.01	380	0.13	0.12	11	337	358.3	0	0
16, July	B	a	52.3	a	700	0.02	350	0.15	0.3	11	11.5	155	0	0
16, July	C	a	62.9	b	400	0.03	333	0.15	0.3	11	20.8	8.3	0	0
16, July	D	a	67.1	a	400	0.04	267	0.15	0.3	11	51.5	32.2	0	0
24, Aug	A	b	44	b	250	0.03	300	0.13	0.12	11	60.2	9.6	0	0
24, Aug	B	a	47.1	b	200	0.03	289	0.13	0.12	11	153.6	8.2	0	0
24, Aug	C	a	50.2	b	200	0.02	311	0.13	0.12	11	111.4	9	0	0
24, Aug	D	a	54.1	a	200	0.03	289	0.13	0.12	11	115.4	8.1	0	0
24, Aug	E	a	57.9	a	200	0.03	267	0.15	0.3	11	87.6	7.7	0	0
24, Aug	F	a	61.4	a	200	0.04	289	0.15	0.3	11	41.3	9.1	0	0
24, Aug	G	a	64.6	b	200	0.05	244	0.15	0.3	11	84.7	7.1	0	0
24, Aug	H	a	68.4	b	200	0.05	222	0.15	0.3	11	67.9	2.6	0	0
25, Aug	A	a	33.4	a	250	0.02	278	0.13	0.12	11	29.2	5.9	0	0
25, Aug	B	a	37.6	a	200	0.02	278	0.13	0.12	11	43.2	9.1	0	0
25, Aug	C	a	40.8	b	200	0.03	311	0.13	0.12	11	32.2	6.1	0	0
25, Aug	D	a	43.9	b	200	0.03	267	0.13	0.12	11	22.5	6.8	0	0
25, Aug	E	a	47	b	200	0.04	289	0.15	0.3	11	31.4	6.3	0	0
25, Aug	F	a	52	b	200	0.04	278	0.15	0.3	11	28.3	4.1	0	0
25, Aug	G	a	54	b	200	0.05	244	0.15	0.3	11	33.4	3.2	0	0
25, Aug	H	a	61.2	b	200	0.05	211	0.15	0.3	11	33.6	5.6	0	0
26, Aug	A	a	37.5	b	250	0.03	289	0.13	0.12	11	70.2	9.2	0	0
26, Aug	B	a	39.6	a	250	0.02	256	0.13	0.12	11	38.3	6.8	0	0
26, Aug	C	a	41.7	b	200	0.02	267	0.13	0.12	11	23	5.9	0	0
26, Aug	D	a	43.8	a	200	0.03	267	0.13	0.12	11	20.3	5.2	0	0
26, Aug	E	a	45.8	b	200	0.04	289	0.15	0.3	11	46.6	5.2	0	0
26, Aug	F	a	49.9	b	200	0.04	278	0.15	0.3	11	57.7	5.5	0	0



26, Aug	G	a	51.9	b	200	0.05	222	0.15	0.3	11	60	5.4	0	0
26, Aug	H	b	62.6	b	200	0.05	211	0.15	0.3	11	21.1	2.1	0	0

---

SNICAR online, <http://snow.engin.umich.edu/>